Magnetic fields in circumstellar disks traced with spectro-polarimetry

G. H.-M. Bertrang[1], S. Wolf[1]

[1]Universität zu Kiel, Institut für Theoretische Physik und Astrophysik, Leibnizstraße 15, 24118 Kiel, Germany

e-mail: gbertrang@astrophysik.uni-kiel.de

Astrophysik Kiel

CAU Christian−Albrechts−Universität zu Kiel
Mathematisch−Naturwissenschaftliche Fakultät

Abstract

Observations of polarized submillimeter radiation from T-Tauri disks potentially enable us to study their magnetic fields. In this context, recent studies show that the anisotropy of the radiation field may have a major influence on the polarized reemission radiation of these disks (Cho & Lazarian, 2007). Based on polarized radiative transfer simulations we aim at modeling, characterizing, and explaining polarimetric observations of T-Tauri disks. For this purpose we apply a modified version of the 3D continuum radiative transfer code MC3D (Wolf+1999, Wolf 2003) that takes the anisotropy of the radiation field into account. We extended the code to allow us to consider dust grain alignment of non-spherical dust grains due to magnetic fields (3D). As grain alignment mechanism we assume radiative torques within a wavelength range of $1-1000\ \mu m$. With this sophisticated polarized radiative transfer code, we are able to model polarized spectral energy distributions and spatially resolved polarization maps of the thermal dust emission of circumstellar disks.

Questions?

The author of this poster is around and happy to answer any question!

1. Polarized Radiative Transfer

The Stokes vector formalism gives one access to the polarization information of the reemission radiation, dependent on the position of the observer ($\theta_{obs}, \varphi_{obs}$). The dust particles are considered to be oblate and perfect black body radiators with the ability to align with the magnetic field by radiative torques (RATs; Cho & Lazarian, 2007). Therefore, the polarized reemission contains the information about the projected magnetic field structure along the line of sight.

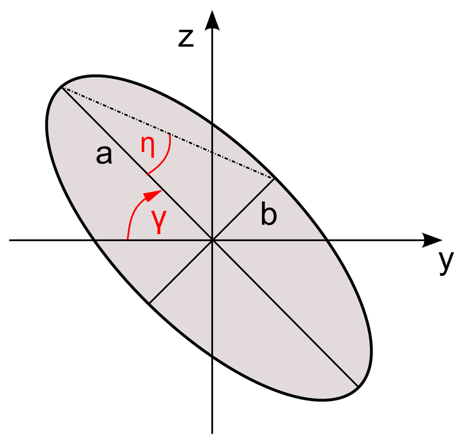

$$I = C_{abs} \cdot B_\lambda(T)$$
$$Q = I \cdot \cos 2\eta \cos 2\gamma$$
$$U = I \cdot \cos 2\eta \sin 2\gamma$$
$$V = I \cdot \sin 2\eta$$
$$|\tan\eta| = b/a = \sin\theta_{obs} \cdot \cos\varphi_{obs}$$

2. Projection Effect on Polarized SEDs

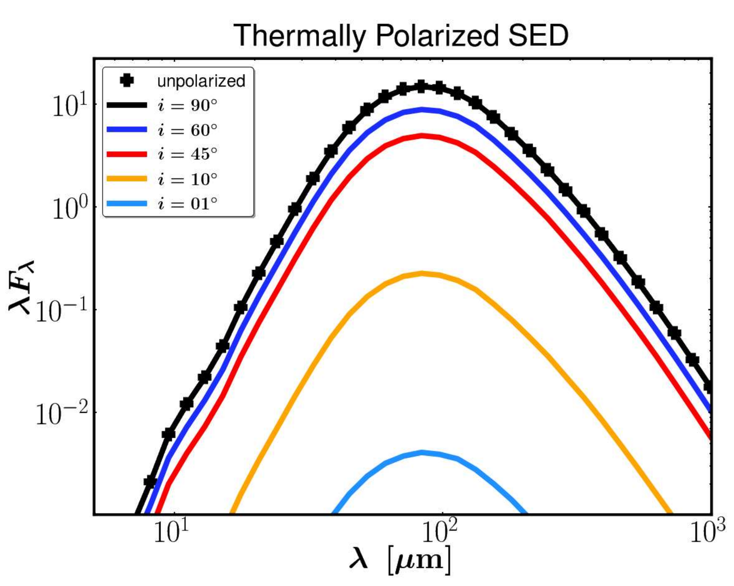

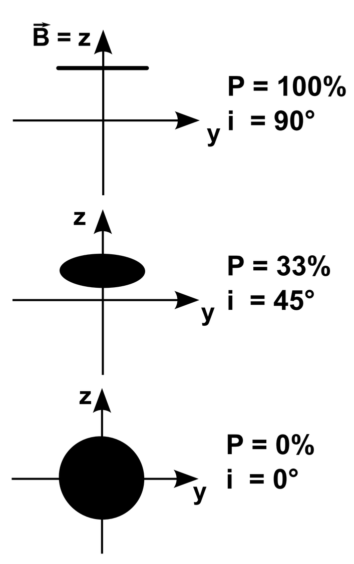

In the case of a spherical dust distribution with perfectly aligned dust grains and a homogenous magnetic field:

$$\rho(r) = r^{-1}, \quad \vec{B} = \vec{e}_z,$$

the only change in the SED at different inclinations i is caused by the projection effect on polarimetry. Analytical tests with this model show a very high accuracy of our simulations.

3. Dust grain alignment by radiative torques (RATs)

In a radiation field, dust grains are put in rotation because of differences in their cross sections for left/right handed polarized radiation (Dolginov & Mitrofanov, 1976). The critical factor here is the angular frequency ratio $(\omega_{\rm rad}/\omega_{\rm th})^2$. Only if $(\omega_{\rm rad}/\omega_{\rm th})^2$ exceeds 10, the dust grains are perfectly aligned to the magnetic field (Cho & Lazarian, 2007). Unlike Cho & Lazarian (2007), we take the anisotropy, $\gamma_{\rm aniso}$, of the radiation field into account.

$$\left(\frac{\omega_{\rm rad}}{\omega_{\rm th}}\right)^2 = 4.72\cdot 10^9 \cdot \frac{\alpha_1}{\delta^2}\cdot \rho_3 \cdot \left(\frac{\gamma_{\rm aniso}\cdot u_{\rm rad}}{n_{\rm H} kT}\right)^2 \cdot \left(\frac{\lambda}{\mu m}\right)^2 \cdot \left(\frac{1}{1+\tau_{\rm drag,gas}/\tau_{\rm drag,em}}\right)^2 \cdot \left(\frac{\lambda}{a}\right)^{-6}$$

α_1, δ: dust grain specific geometrical factors; $\gamma_{\rm aniso}$: anisotropy of the radiation field; u_{rad}: spectral energy density; $\tau_{\rm drag,gas}/\tau_{\rm drag,em}$: ratio of gas drag to thermal emission drag times.

4. Our model

Dust density distribution (Shakura & Sunyaev, 1973)

$$\rho(r,z) \sim \left(\frac{r_0}{r}\right)^\alpha \exp\left(-\frac{1}{2}\left[\frac{z}{h_0}\left(\frac{r_0}{r}\right)^\beta\right]^2\right)$$

α	β	h_0	r_0	$M_{\rm gas}/M_{\rm dust}$	$R_{\rm in}$	$R_{\rm out}$	dist.
1.2	1.14	10 AU	100 AU	100	0.01 AU	100 AU	140 AU

MRN dust: $a \in [0.01, 1000]\ \mu$m; $M_{\rm d} = 10^{-6}\ {\rm M}_\odot$

Star: $R_* = 2.5\ R_\odot$; $T_* = 5500$ K

Magnetic field structure: toroidal; Dust grain alignment: RATs

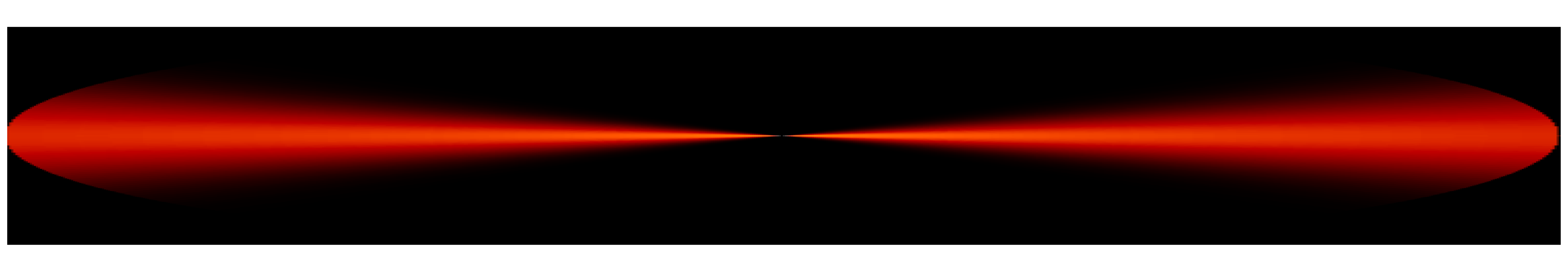

Dust density distribution perpendicular to the disk midplane.

5. Dust grain alignment within the disk

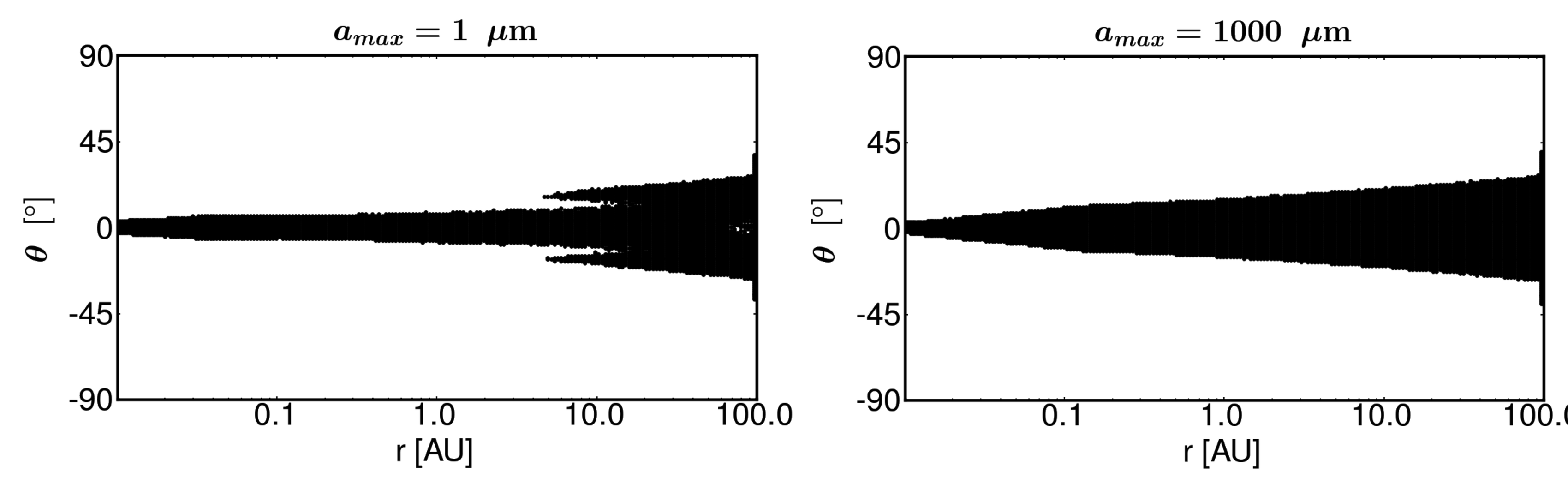

Aligned dust grains in the disk plane perpendicular to the disk midplane are shown here in black.

Dust grain alignment depends not only on the local radiation field, but also on the local density and dust grain size. The impact of the maximum grain size is shown here. Since larger dust grains have larger temperatures, it is expected that larger particles get aligned much more efficiently, consistend with our results.

6. Polarized SEDs with aligned dust grains

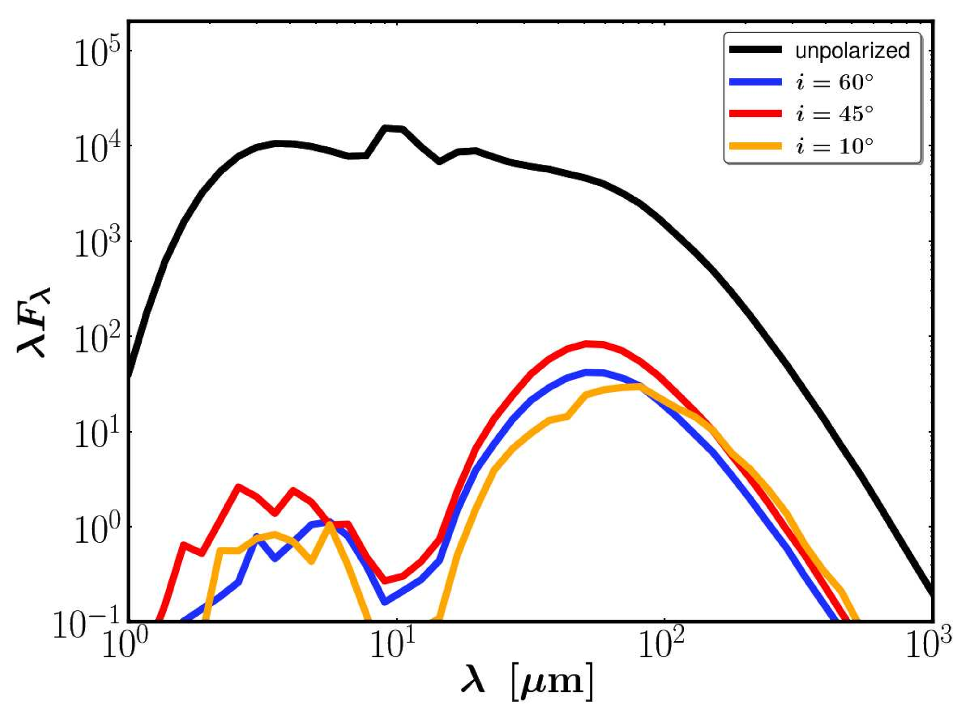

Unpolarized SEDs vs. SEDs of polarized radiation

$\mathbf{a_{max} = 1\ \mu m}$

In the case of small dust grains ($a_{\rm max} = 1\ \mu$m) the dust grain alignment is the most important factor for the shape of the polarized SED.

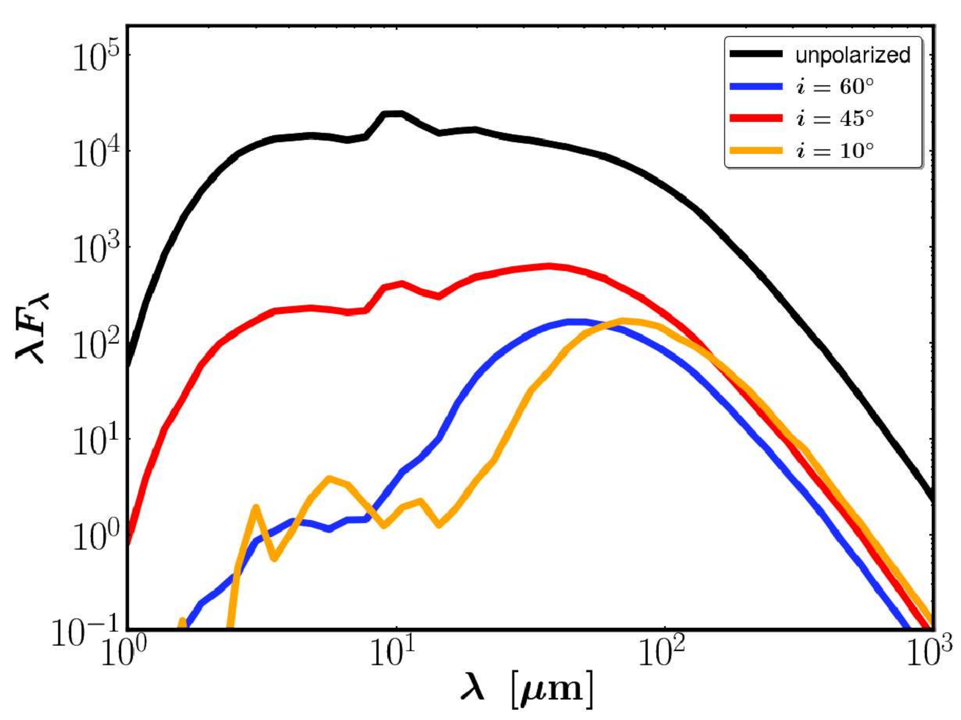

$\mathbf{a_{max} = 1000\ \mu m}$

In the case of large dust grains ($a_{max} = 1000\ \mu$m) the dust grain alignment has a higher impact on the polarized SED very close ($i = 60°$) and far off ($i = 10°$) the disk midplane. Along disk layers with moderate density and radiative anisotropy, the dust grain alignment is high enough over a large wavelength interval and the projection effect on polarimetry dominates the SED shape.

By applying dust grain alignment and inclination dependent projection effects on non-spherical dust grains, dust grain sizes are clearly distinguishable for a given dust density distribution and magnetic field configuration.

7. Conclusion

- Our code considers the projection effect on polarimetry with high accuracy.
- The dust grain alignment can be distinguished for different grain sizes.
- SEDs of polarized radiation show sensitivity for grain alignment, grain sizes and inclinations.

References Cho, J. and Lazarian, A., 2007, *ApJ*, 669:1085. Dolginov, A. Z. and Mitrofanov, I. G., 1976, *APSS*, 43:291. Shakura, N. I. and Sunyaev, R. A., 1973, *A&A*, 24:337. Wolf, S., 2003, *Computer Physics Communications*, 150:99. Wolf, S., Henning, Th., and Stecklum, B., 1999, *A&A*, 349:839.